Mean-field approximation for spacing distribution functions in classical systems

Diego Luis González,[1,*] Alberto Pimpinelli,[1,2,†] and T. L. Einstein[1,‡]

[1]*Department of Physics, University of Maryland, College Park, Maryland 20742-4111, USA*
[2]*French Embassy, Consulate General of France, Houston, Texas 77056, USA*

We propose a mean-field method to calculate approximately the spacing distribution functions $p^{(n)}(s)$ in one-dimensional classical many-particle systems. We compare our method with two other commonly used methods, the independent interval approximation and the extended Wigner surmise. In our mean-field approach, $p^{(n)}(s)$ is calculated from a set of Langevin equations, which are decoupled by using a mean-field approximation. We find that in spite of its simplicity, the mean-field approximation provides good results in several systems. We offer many examples illustrating that the three previously mentioned methods give a reasonable description of the statistical behavior of the system. The physical interpretation of each method is also discussed.

PACS number(s): 05.40.−a, 68.55.A−, 68.35.−p, 81.15.Aa

I. INTRODUCTION

The spacing distribution functions $p^{(n)}(s)$ are often used to describe the statistical behavior of many-particle systems in one dimension (1D) [1–7]. By definition, $\hat{p}^{(n)}(S)$ is the probability density that an interval of length S which starts at a particle contains exactly n particles and that the next, the $(n+1)$-th particle, is in $[S,S+dS]$. The relative spacing is defined as $s = S/\langle S \rangle$, where $\langle S \rangle$ is the average of S. However, the $p^{(n)}(s)$ are also used in other contexts. For example, in 1D systems with domains, S represents the spacing between domain boundaries [8–15], while in random-matrix theory and quantum systems this variable represents the spacing between adjacent energy eigenvalues [16–21]. In the physics of surfaces, S can be the distance between islands in epitaxial growth models or the terrace width between adjacent steps on vicinal (misoriented) surfaces [22–25].

The spacing distribution functions are useful even in nonequilibrium systems having dynamical scaling. One such system is the coalescing random walk (CRW). In CRW, all particles execute independent random walks, suffering a fusion reaction $(A + A \rightarrow A)$ when two particles meet. Clearly, in this system the number of particles and $\langle S(t) \rangle$ are time dependent. Despite this, it is possible to define a scaled spacing distribution according to

$$p^{(n)}(s) = \langle S \rangle \, \hat{p}^{(n)}(s \, \langle S \rangle, t). \tag{1}$$

Since the $p^{(n)}(s)$ in Eq. (1) do not depend on t, they can be compared with the spacing distribution functions of an equilibrium system. More information about the CRW is given in Ref. [26].

In this paper, we propose a mean-field model to calculate in an approximate way the spacing distribution functions of classical many-particle systems. Our method is compared with other existing methods commonly used to calculate $p^{(n)}(s)$. These approximate methods are important because they are often used to obtain the spacing distribution functions for systems where the exact analytical solution either cannot

be obtained or, if it is obtained, cannot be handled easily because of its complexity. In Sec. II, we provide a brief introduction to the spacing distribution functions, giving some important definitions. In Secs. III and IV, we briefly review the independent interval approximation (IIA) and the extended Wigner surmise (EWS) [27], respectively. (Note that the EWS differs [27] from the so-called generalized Wigner surmise (GWS) [22–24], which is not used in this paper.) In Sec. V, we develop two mean-field models. In each case, we provide several examples of the use of these methods, analyzing their advantages and limitations. Finally, Sec. VI presents our conclusions.

All our numerical data for Dyson's Brownian motion model were generated with a Monte Carlo simulation that uses the standard METROPOLIS algorithm. We used a lattice having $L = 10\,000$ sites with $N = 50$ particles. The statistics take into account over 20 000 realizations.

II. BASIC DEFINITIONS

Consider N particles which can move around a circle of circumference L; periodic boundary conditions are imposed, that is, $x_{N+j} = x_j$, where x_j is the position of the jth particle. If the system is in equilibrium at an inverse temperature β, then its statistical behavior is totally defined by the joint probability distribution $P_N(x_1, \ldots, x_N; \beta)$

$$P_N(x_1, \ldots, x_N; \beta) = \frac{1}{Z_N(L; \beta)} e^{-\beta \, V(x_1, \ldots, x_N)}, \tag{2}$$

where $V(x_1, \ldots, x_N)$ is the total interaction energy among the N particles and Z_N is the configurational partition function of the system. Then $P_N(x_1, \ldots, x_N; \beta)$ represents the probability density to find particle 1 in $[x_1, x_1 + dx_1]$, particle 2 in $[x_2, x_2 + dx_2]$, etc. In practice, this joint probability distribution cannot be obtained easily from experiments or numerical simulations because it depends on many variables. Instead, one usually evaluates the spacing distribution functions $\hat{p}^{(n)}(S)$, where $n \geqslant 0$. Each $\hat{p}^{(n)}(S)$ contains reduced information about the system. In order to have a more complete description of the statistical behavior of the system, it is necessary to know $\hat{p}^{(n)}(S)$ for all n. From them, it is possible to calculate the pair

*dgonzal2@umd.edu
†apimpin1@umd.edu
‡einstein@umd.edu

correlation function $g(s)$ by using the expression

$$g(s) = \sum_{n=0}^{\infty} p^{(n)}(s). \tag{3}$$

The sum in Eq. (3) seems to be a formidable task. However, in many cases $g(s)$ quickly relaxes to 1; therefore, just the first few $p^{(n)}(s)$ have to be calculated explicitly. Many thermodynamic quantities can be expressed in terms of the pair correlation function and the interaction potential between particles [28,29].

When the N particles interact via a pair potential $v(r)$, the total energy of interaction reduces to

$$V(x_1, \ldots, x_N) = \sum_{m=1}^{N} \sum_{j=1}^{q} v(x_{m+j} - x_m), \tag{4}$$

with q the number of interacting neighbors. For $q = 1$, we have nearest-neighbor interactions and for $q = N - 1$ each particle interacts with all other particles. We henceforth denote the latter as "full-range" interactions, corresponding to infinite range in the thermodynamic limit. As mentioned previously, the probability density to find the N particles around the positions $x_1, \ldots, x_N$ is given by Eq. (2). As usual, Z_N can be calculated from

$$Z_N(L; \beta) = \int dx_1 \ldots dx_N \, \delta(\Lambda) \, P_N(x_1, \ldots, x_N; \beta), \tag{5}$$

where $\Lambda = L - \sum_{i=1}^{N} (x_{i+1} - x_i)$. Making the change of variables $S_i = x_{i+1} - x_i$, the partition function takes the form

$$Z_N(L; \beta) = \int dS_1 \ldots dS_N \, \delta(\Lambda) \, P_N(S_1, \ldots, S_N; \beta), \tag{6}$$

now with $\Lambda = L - \sum_{i=1}^{N} S_i$. In the same way, the joint probability distribution can be written as

$$P_N(S_1, \ldots, S_N; \beta) = \frac{1}{Z_N(L; \beta)} e^{-\beta \Omega}, \tag{7}$$

with

$$\Omega = \sum_{m=1}^{N} [v(S_m) + v(S_m + S_{m+1}) + \cdots + v(S_m + \cdots + S_{m+q-1})]. \tag{8}$$

Taking $f(S; \beta) \equiv f(S) = e^{-\beta v(S)}$, we find

$$P_N(S_1, \ldots, S_N; \beta) = \frac{1}{Z_N(L; \beta)} \prod_{m=1}^{N} F(S_m, \ldots, S_{m+q-1}), \tag{9}$$

where we define $F(S_m, \ldots, S_{m+q-1}) = f(S_m) f(S_m + S_{m+1}) \cdots f(S_m + \cdots + S_{m+q-1})$. The joint probability distribution of n consecutive spacings $P_n(S_1, \ldots, S_n; \beta)$ is given by

$$P_n(S_1, \ldots, S_n; \beta) = \int dS_{n+1} \ldots dS_N \, P_N(S_1, \ldots, S_N; \beta). \tag{10}$$

By definition, the nth spacing distribution function $\hat{p}^{(n)}(S) \equiv \hat{p}^{(n;q)}(S)$ can be written as

$$\hat{p}^{(n;q)}(S) = \int_0^{\infty} dS_1 \ldots dS_{n+1} \, \delta(\eta) \, P_{n+1}(S_1, \ldots, S_{n+1}; \beta), \tag{11}$$

with $\eta = S - \sum_i^{n+1} S_i$. Note that this notation makes explicit the dependence of the spacing distributions on the number of interacting neighbors q. The average spacing between particles is $\langle S \rangle = L/N$. Then, the scaled probability density is

$$p^{(n;q)}(s) = \int_0^{\infty} dS_1 \ldots dS_{n+1} \, \delta(\lambda) P_{n+1}(S_1, \ldots, S_{n+1}; \beta), \tag{12}$$

with $\lambda = \eta / \langle S \rangle$. Note that Eq. (12) satisfies the normalization conditions [17]

$$\int_0^{\infty} ds \, p^{(n;q)}(s) = 1 \quad \text{and} \quad \int_0^{\infty} ds \, s \, p^{(n;q)}(s) = n + 1. \tag{13}$$

In general, the integral given in Eq. (12) cannot be easily calculated by analytical methods. In fact, it can be solved in just a few cases. A simple example of this is given by the potential $v(r) = -\ln(r)$ with $q = 1$. By using the Laplace transform method, it can be shown [1,18] that

$$p^{(n;1)}(s; \beta) = \frac{(1+\beta)^{(1+\beta)(1+n)}}{\Gamma[(1+\beta)(1+n)]} s^{\beta+n(1+\beta)} e^{-s(1+\beta)}. \tag{14}$$

The case $q = N - 1 \to \infty$ was solved by Dyson and so is termed the Dyson's Brownian motion model [30,31]. The general case, $1 < q < N - 1$, with $N, L \to \infty$ was solved in Ref. [1] through integral equations. Henceforth, we denote as Dyson's Brownian model a 1D system in which the particles interact through a logarithmic potential, regardless of the range of interaction q.

III. INDEPENDENT INTERVAL APPROXIMATION

A. General formalism

The easiest method to obtain approximate expressions for $p^{(n;q)}(s)$ is the independent interval approximation (IIA). In the IIA, all spacing distributions are generated from the nearest-neighbor distribution $p^{(0;q)}(s)$. The essence of the approach is to neglect the correlations between the sizes of adjacent spacings. Consequently, the probability of finding particles around positions $x_1, x_2, \ldots, x_N$ is given by

$$P_N^{\text{eff}}(x_1, x_2, \ldots, x_N; \beta) = \prod_{i=1}^{N} p^{(0;q)}(x_{i+1} - x_i)$$
$$= e^{-\beta \sum_{i=1}^{N} v_{\text{eff}}(x_{i+1} - x_i)}. \tag{15}$$

Comparing Eq. (15) with the Boltzmann factor given in Eq. (2), we conclude that

$$V(x_1, \ldots, x_N) + C = \sum_{i=1}^{N} v_{\text{eff}}(x_{i+1} - x_i). \tag{16}$$

The constant C is needed to ensure normalization of the joint probability distribution.

In IIA, each particle is taken to interact with its nearest neighbors via an effective pair potential given by $v_{\text{eff}}(r) =$

$-\ln[p^{(0;q)}(r)]$. This effective potential is generally different from the real potential; most importantly, the effective potential usually depends on the inverse temperature of the studied system. Note that the IIA reproduces exactly the functional form of the interaction potential $V(x_1, \ldots, x_N)$ in the case of $q = 1$. However, we caution that entropic repulsions (arising from fermionic noncrossing interactions such as occur in the terrace-step-kink (TSK) model of steps discussed in Sec. V C) intrinsically involve all particles; hence, this part of $V(x_1, \ldots, x_N)$ in Eq. (16) cannot be decomposed exactly into components between neighboring parts.

B. Applications

As a sample application of the IIA, consider Dyson's Brownian model with $q = 1$. From Eq. (12), the statistical behavior of this model is clearly equivalent to that in which particles interact only with their nearest neighbors through an effective pair potential given by

$$v_{\text{eff}}(r) = -\ln(r) + \frac{(1+\beta)}{\beta}r + C. \tag{17}$$

In Eq. (17), the first term represents the repulsive force between adjacent particles, while the second takes into account the effect of the average force on the ends of the interval of length r due to the particles which are outside the interval. In the IIA, the statistical behavior of Dyson's Brownian motion model with nearest-neighbor interactions is given by

$$P_N^{\text{eff}}(x_1, x_2, \ldots, x_N; \beta) = C^N \prod_{j=1}^{N} e^{\beta \ln(S_j) - (1+\beta)S_j}. \tag{18}$$

From this discussion, it should be clear that many systems can share the same statistical behavior even when they have different interaction potentials between particles. In the above example, the real and effective systems have the same statistical behavior but their interaction potentials differ.

As for all systems with just nearest-neighbor interactions, in the IIA all spacing distribution functions can be calculated analytically in Laplace space [1,2]. This approximation should work properly in systems with short-range interactions between particles because the correlations between the sizes of adjacent spacings are usually weak compared to the case of long- or infinite-range interactions.

Consider again Dyson's Brownian motion model. By integrating Eq. (18) we see that, for $q = 1$, the IIA describes exactly the statistical behavior of this system. Figure 1(a) shows that the IIA is also a good approximation for $q = 2$. The functions plotted in Fig. 1(a) were calculated from the exact expression for $p^{(0;2)}(s)$ given in Ref. [1] for $q = 2$

$$p^{(0;2)}(s) = s \left(2.4773 + 6.0681\,s + 3.7159\,s^2\right) e^{-3s}, \tag{19}$$

via Eqs. (12) and (15). In this case, the exact expression for $p^{(1;2)}(s)$ is given by

$$p^{(1;2)}(s) = s^4 \left(2.5054 + 3.068\,s + 0.7516\,s^2\right) e^{-3s}, \tag{20}$$

while in the IIA we have the result

$$\begin{aligned} p^{(1;2)}(s) = s^3 \big(&1.02247 + 2.50462s + 2.14728s^2 \\ &+ 0.751391s^3 + 0.0986s^4\big) e^{-3s}. \end{aligned} \tag{21}$$
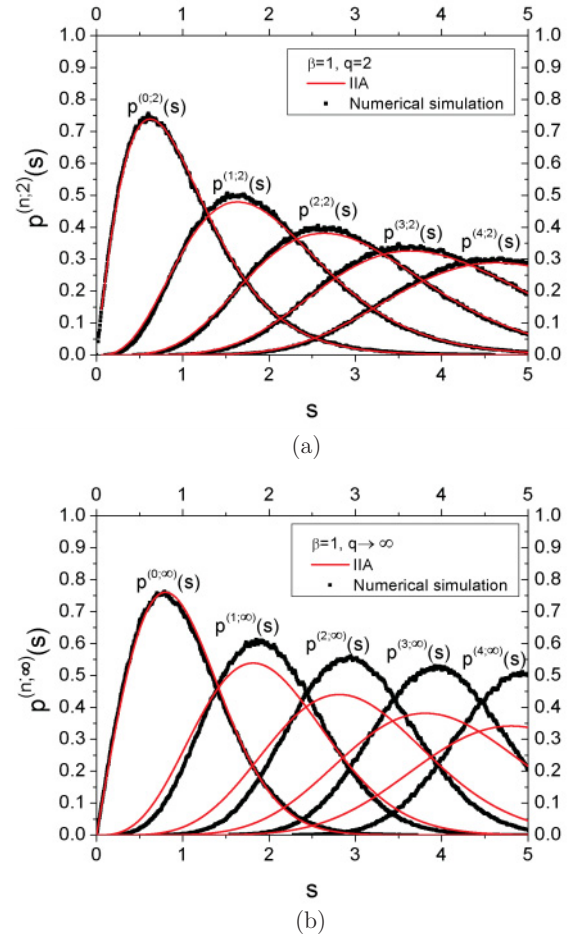

FIG. 1. (Color online) The IIA for Dyson's Brownian motion model with (a) $q = 2$ and (b) $q = 49$.

We conclude that the IIA reproduces the $p^{(1;2)}(s) \propto e^{-3s}$ behavior of the spacing distribution functions for large values of s but fails for small values of s, predicting $p^{(1;2)}(s) \propto s^3$ rather than the exact result $p^{(1;2)}(s) \propto s^4$.

However, as q increases the IIA becomes very poor, as shown in Fig. 1(b), where we took the widely used Wigner surmise expression for $q = N - 1 \to \infty$,

$$p^{(0;\infty)}(s) = \frac{\pi}{2}s\,e^{-\frac{\pi}{4}s^2}, \tag{22}$$

and calculated $p^{(n;\infty)}(s)$ from Eqs. (12) and (15). As expected from the lack of correlation, the IIA becomes a progressively poorer approximation as n increases.

Another example of a system in which the IIA can be applied successfully is the point island model for epitaxial growth [25,32–35]. In this model, the monomers are deposited at random on a d-dimensional lattice. The monomers diffuse across the lattice until reaching a site occupied by another monomer, at which point an island is formed. This coalescing process is called nucleation. While the monomers are mobile, the islands remain static and do not grow laterally. Figure 2 shows that the IIA is a good approximation for this model. In Fig. 2(a), we use the heuristic equation $p^{(0;\infty)}(s) = A_\alpha s^\alpha e^{-B_\alpha s^2}$ with $\alpha = \frac{3}{2}$ given in Ref. [33], while in Fig. 2(b)
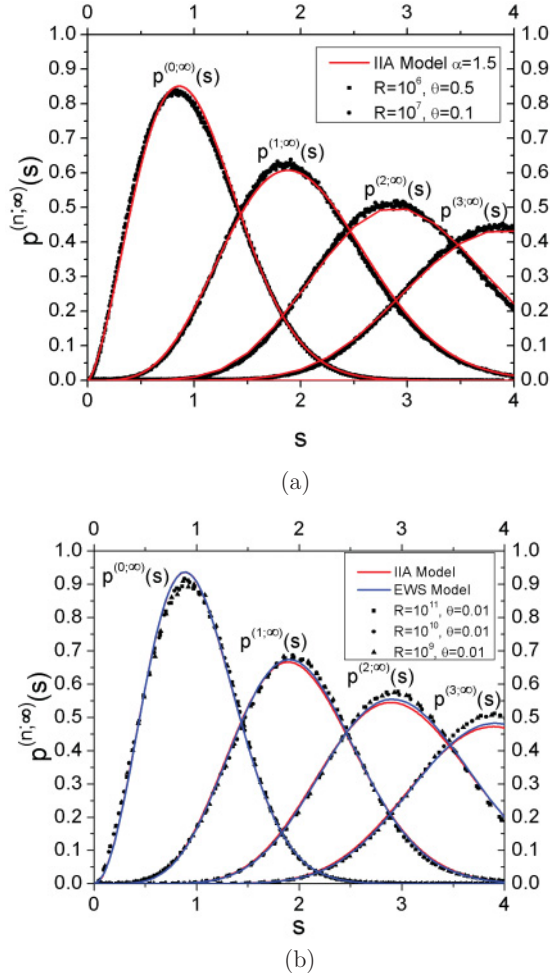
FIG. 2. (Color online) The IIA for the point island model of epitaxial growth for (a) $d = 1$ and (b) $d = 2$. We also show the EWS approximation for this model in the two-dimensional (2D) case.

we use the same expression but with $\alpha = 2$ [36]. Additional examples of the IIA can be found in Refs. [12,15,37].

In short, in the IIA the statistical behavior of an N-particle system is modeled by using another system whose particles interact through an effective potential with their nearest neighbors. The effective potential is a function of the inverse temperature and must be calculated for each particular system. However, as shown in Refs. [12] and [15], $p^{(0;q)}(s)$ does not uniquely define the system.

IV. EXTENDED WIGNER SURMISE

The exact expression for the spacing distribution functions for Dyson's Brownian motion model with full-range interactions is complicated and unwieldy. However, Wigner proposed accurate and simple expressions for $p^{(0;\infty)}(s)$ in the special cases of $\beta = 1$, 2, and 4. Abul-Magd and Simbel [17] subsequently extended Wigner's surmise to $n > 0$ by making the ansatz

$$p^{(n+1;\infty)}(s) \underset{s \to 0}{\propto} s^{(n+1)\beta} \int_0^s p^{(n;\infty)}(s), \qquad (23)$$

using Wigner's expressions for $p^{(0;\infty)}(s)$, and assuming Gaussian decay. In this extended Wigner surmise (EWS), $p^{(n;\infty)}(s)$ for Dyson's Brownian model with $q = N - 1 \to \infty$ is written as

$$p^{(n;\infty)}(s) = A_n s^{\alpha_n} e^{-B_n s^2}, \qquad (24)$$

with $\alpha_n = n + (n + 1)(n + 2)\beta/2$. The constants A_n and B_n are calculated from the normalization conditions given in Eq. (13). In the EWS, the functions $p^{(n;\infty)}(s)$ are completely described by their behavior in the two limits $s \to 0$, where $p^{(n;\infty)}(s) \propto s^{\alpha_n}$, and $s \to \infty$, where $p^{(n;\infty)}(s) \propto e^{-B_n s^2}$.

As mentioned above, the EWS was developed to find analytical expressions for the spacing distributions of Dyson's Brownian motion model. Nonetheless, it can also be applied to a great variety of systems with the suitable choice of α_n. One advantage of the EWS compared to alternatives like the IIA is its mathematical simplicity. Another is that the IIA is well defined only for 1D systems, while the EWS does not make any assumptions about the geometry of the system and it can be applied to more general systems. In Fig. 2(b), we have applied the IIA simply as a mathematical artifact for a 2D case; in this case, it is not possible to define spacings between islands.

Figure 2(b) shows that the Wigner surmise is a good approximation for the point island model for epitaxial growth with $d = 2$. For Dyson's Brownian motion model with infinite-range interactions, the EWS for $n = 0$ is accurate to 5% for $\beta = 1$ and even better for $\beta = 2$ or 4 [24,38]. For $n > 0$, the fits visually seem to have the same quality as for $n = 0$ [12,17]. In the IIA, all $p^{(n;q)}(s)$ can be calculated in Laplace space, but the inverse of those expressions usually cannot be calculated for large values of n. For the point-island model ($d = 2$) in the EWS, we invoke Eq. (24) as the ansatz and calculate α_n from a simple argument: Since we know that the IIA gives a good fit for this model, we can expect that for $s \ll 1$

$$p^{(n;\infty)}(s) \approx \int_0^\infty ds_1 \ldots \int_0^\infty ds_{n+1} \prod_{i=1}^{n+1} p^{(n;\infty)}(s_i) \propto s^{3n+2}, \qquad (25)$$

so that $\alpha_n = 3n + 2$ [36]. In Fig. 2(b), we see that the differences between the IIA and the EWS are almost imperceptible for the point island model in $d = 2$.

Unfortunately, the EWS is not always a good approximation. For example, consider the CRW and Dyson's Brownian model with infinite range of interactions and $\beta = 1$. In Ref. [39], it was shown that both systems have Gaussian behavior for large values of s and that α_n is given in Eq. (24), with $\beta = 1$, for both systems. However, the EWS gives good results for Dyson's Brownian motion model but not for the CRW.

Another example is Dyson's Brownian motion model with $1 < q < N - 1$, where $p^{(n;q)}(s) \propto e^{-B_n s}$ for $s \to \infty$ [1]. It is then tempting to extend our previous approach by writing $p^{(n;q)}(s)$ in the more general form

$$p^{(n;q)}(s) = A_n s^{\alpha_n} e^{-B_n s^\gamma}, \qquad (26)$$

here with $\gamma = 1$, while α_n is unchanged from Eq. (24). In fact, for finite-range interactions, the functions $p^{(n;q)}(s)$ have the form

$$p^{(n;q)}(s) = A_n s^{\alpha_n} Q_n(s) e^{-B_n s}, \qquad (27)$$

where $Q_n(s)$ is a polynomial whose degree depends on n and β [1]. Thus, for Dyson's Brownian motion model with finite-range interactions, the spacing distribution functions cannot be described solely by their behavior in the limits $s \to 0$ and $s \to \infty$; the behavior of $p^{(n;q)}(s)$ for intermediate values of s is clearly important.

Additional applications of the EWS can be found in Ref. [39], where the EWS was applied to study the statistical behavior of an N particles system with nearest-neighbor interaction $v(r) = \frac{\pi}{4}r^2 - \ln(\frac{\pi}{2}r)$. In this case, the EWS gives excellent results for $\gamma = 2$ and $\alpha_n = 2\,n + 1$. This potential was used to model two $d = 1$ nonequilibrium systems with domain formation [12].

V. MEAN-FIELD MODEL

In Refs. [22] and [23], a mean-field model is proposed to obtain an analytical expression for the distribution of terrace widths (spacings between adjacent steps) on vicinal surfaces. Following these ideas, we propose a new approximate description for Dyson's Brownian motion model with finite-range interactions, that is, for arbitrary values of q. This system was solved exactly in Ref. [1]. However, the expressions found there for the spacing distribution function in the range $1 < q < N$ are unwieldy because they involve integral equations which increase in difficulty for large values of q and β. Rather (and following Refs. [22] and [23]), we propose a mean-field approximation to obtain simple expressions for this model.

A. Nearest-neighbor distribution with finite-range interaction

1. Simple mean-field approximation (SMF)

According to the logarithmic potential proposed by Dyson, the force $F_m \equiv F_m(x_1, \ldots, x_N)$ on the mth particle is given by

$$F_m = \sum_{j=1}^{q} \left(\frac{1}{x_{m+j} - x_m} - \frac{1}{x_m - x_{m-j}} \right). \quad (28)$$

Consequently, the deterministic damped-oscillator equation for the mth particle is

$$M \frac{d^2 x_m}{dt^2} = -\frac{2}{\Gamma} \frac{dx_m}{dt} + F_m. \quad (29)$$

where $2/\Gamma$—anticipating the subsequent development—is the friction coefficient. In the overdamped limit of strong friction, the system relaxes quickly to equilibrium, allowing us to take $d^2 x_m/dt^2 = 0$ and rewrite Eq. (29) as first-order differential equations

$$\frac{dx_m}{dt} = \frac{\Gamma}{2} F_m. \quad (30)$$

As in Ref. [40], we then consider the time evolution of the spacings between adjacent particles, $S_m = x_{m+1} - x_m$, adding a stochastic term to produce the set of Langevin equations

$$\frac{dS_m}{dt} = \frac{\Gamma}{2}(F_{m+1} - F_m) + \frac{\Gamma}{2}\eta_m(t), \quad (31)$$

where the $\eta_m(t)$ introduce Gaussian white noise for each spacing, and

$$F_{m+1} - F_m = \frac{1}{\sum_{i=1}^{j} S_{m+i}} - \frac{1}{S_m + \sum_{i=1}^{j-1} S_{m-i}}$$
$$- \frac{1}{S_m + \sum_{i=1}^{j-1} S_{m+i}} + \frac{1}{\sum_{i=1}^{j} S_{m-i}}. \quad (32)$$

Taking the average $\langle\ \rangle$ in Eq. (31) as discussed in Appendix A, we have

$$\frac{dS}{dt} = C_1 \Gamma \sum_{j=1}^{q} \frac{1}{j\,\langle S \rangle} - C_2 \Gamma \sum_{j=1}^{q} \frac{1}{S + (j-1)\langle S \rangle}, \quad (33)$$

where the C_j's are constants which can be interpreted as the renormalization of the strength of interaction. The first sum at the right of Eq. (33) can be calculated easily,

$$\frac{dS}{dt} = \frac{C_1 \Gamma}{\langle S \rangle} H_p - C_2 \Gamma \sum_{j=1}^{q} \frac{1}{S + (j-1)\langle S \rangle}, \quad (34)$$

where $H_q = \sum_{m=1}^{q} m^{-1}$ is the generalized harmonic number of order q. After the change of variables $\tau = \Gamma t/\langle S \rangle^2$ and $s = S/\langle S \rangle$, it is straightforward to show

$$\frac{ds}{d\tau} = C_1 H_q - C_2 \sum_{j=1}^{q} \frac{1}{s + (j-1)}. \quad (35)$$

Then the effective potential associated with Eq. (35) is

$$v_{\text{eff}}(s) = C_1 H_q s - C_2 \sum_{j=1}^{q} \ln[s + (j-1)] + C_3, \quad (36)$$

The nearest-neighbor distribution $p^{(0;q)}(s)$ is given by

$$p^{(0;q)}(s) = A \prod_{j=1}^{q} [s + (j-1)]^{\beta C_2}\, e^{-\beta C_1 H_q s}. \quad (37)$$

The constant C_2 can be calculated by using the fact that for low densities $p^{(0;q)}(s) \approx e^{-\beta v(s)}$, which leads to $C_2 = 1$. The remaining constants can be calculated by using the normalization conditions. In the SMF model, Eq. (37) has a similar functional form to Eq. (27). However, the order of the polynomial factor is not the same in both cases. For example, for the case of $q = 2$ and $\beta = 1$, the SMF model gives

$$p^{(0;2)}(s) \approx 3.30\, s\, (1 + s)\, e^{-2.45s}, \quad (38)$$

which clearly differs from Eq. (19).

2. Improved mean-field approximation

We expect that for large values of q the SMF approximation begins to fail. The reason is that implicit in Eq. (32) there are more terms which depend on S_m. For example, in the case $q = 2$ we have such terms as

$$\frac{1}{x_{m+2} - x_{m+1}} - \frac{1}{x_{m+2} - x_m} = \frac{S_m}{S_{m+1}(S_m + S_{m+1})}, \quad (39)$$

which clearly depend on S_m. The number of such terms increases with q. Furthermore, for full interactions between all pairs of particles, Eq. (37) does not reproduce the behavior of the Wigner surmise. Consequently, we must formulate

an improved mean-field approximation (IMF). After some algebra, it is possible to write Eq. (31) as

$$
\frac{dS_m}{dt} = \frac{\Gamma}{2} \sum_{j=1}^{q-1} \frac{S_m}{(x_{m+j+1} - x_{m+1})(x_{m+j+1} - x_m)}
$$

$$
+ \frac{\Gamma}{2} \sum_{j=1}^{q-1} \frac{S_m}{(x_m - x_{m-j})(x_{m+1} - x_{m-j})}
$$

$$
+ \frac{\Gamma}{2} \left(\frac{1}{x_{m+q+1} - x_{m+1}} + \frac{1}{x_m - x_{m-q}} \right)
$$

$$
- \frac{\Gamma}{x_{m+1} - x_m} + \frac{\Gamma}{2} \eta_m(t). \qquad (40)
$$

By taking the average $\langle \rangle$ in Eq. (40) as discussed in the Appendix A, we find

$$
\frac{dS}{dt} = \Gamma \sum_{j=1}^{q-1} \frac{\tilde{C}_1 S}{j(j+1)\langle S^2 \rangle} + \frac{\Gamma \tilde{C}_1}{q \langle S \rangle} - \frac{\Gamma \tilde{C}_2}{S}. \qquad (41)
$$

where the constants $\tilde{C}_1$ and $\tilde{C}_2$ are defined implicitly in Appendix A. After the changes of variables $\tau = \Gamma t / \langle S \rangle^2$ and $s = S/\langle S \rangle$ and then using $\sum_{j=1}^{q-1} [j(j+1)]^{-1} = (q-1)/q$, it is straightforward to show

$$
\frac{ds}{dt} = \tilde{C}_1 \left(\frac{q-1}{q} \right) \frac{s}{\langle s^2 \rangle} + \frac{\tilde{C}_1}{q} - \frac{\tilde{C}_2}{s} + \eta. \qquad (42)
$$

Then, the effective potential associated with Eq. (42) is

$$
v_{\text{eff}}(s) = -\tilde{C}_2 \ln(s) + \frac{\tilde{C}_1}{2} \left(\frac{q-1}{q} \right) \frac{s^2}{\langle s^2 \rangle} + \frac{\tilde{C}_1}{q} s + C. \qquad (43)
$$

Again, using $p^{(0;q)}(s) \approx e^{-\beta v(s)}$ it is easy to find $\tilde{C}_2 = 1$. The nearest-neighbor distribution $p^{(0;q)}(s)$ is given by

$$
p^{(0;q)}(s) = A s^\beta \exp\left[-\beta \frac{\tilde{C}_1}{2} \left(\frac{q-1}{q} \right) \frac{s^2}{\langle s^2 \rangle} - \beta \frac{\tilde{C}_1}{q} s \right]. \qquad (44)
$$

In the case of full-range interactions, the nearest-neighbor distribution can be written as

$$
p^{(0;q)}(s) = A s^\beta e^{-(\beta \tilde{C}_1/2)(s^2/\langle s^2 \rangle)}. \qquad (45)
$$

By using the normalization conditions, one can show that Eq. (45) is equivalent to the Wigner surmise described by Eq. (24) for $n = 0$. In the case of nearest-neighbor interactions, Eq. (44) takes the form of Eq. (14). For $q > 1$, Eq. (44) predicts a Gaussian tail for large values of s instead of the exponential in Eq. (27). Despite this discrepancy with the exact result, it is reasonable to expect that the IMF model given by Eq. (44) leads to good results, especially for large and small values of q [where it reduces to the Wigner surmise and to Eq. (14), respectively].

Before generalizing our mean-field models to $n > 0$, we offer some comments about Eq. (44). First, as mentioned before, the IMF for the case of full-range interactions was used previously [22,23] to describe the terrace-width distribution between steps on vicinal surfaces. However, Eq. (44)
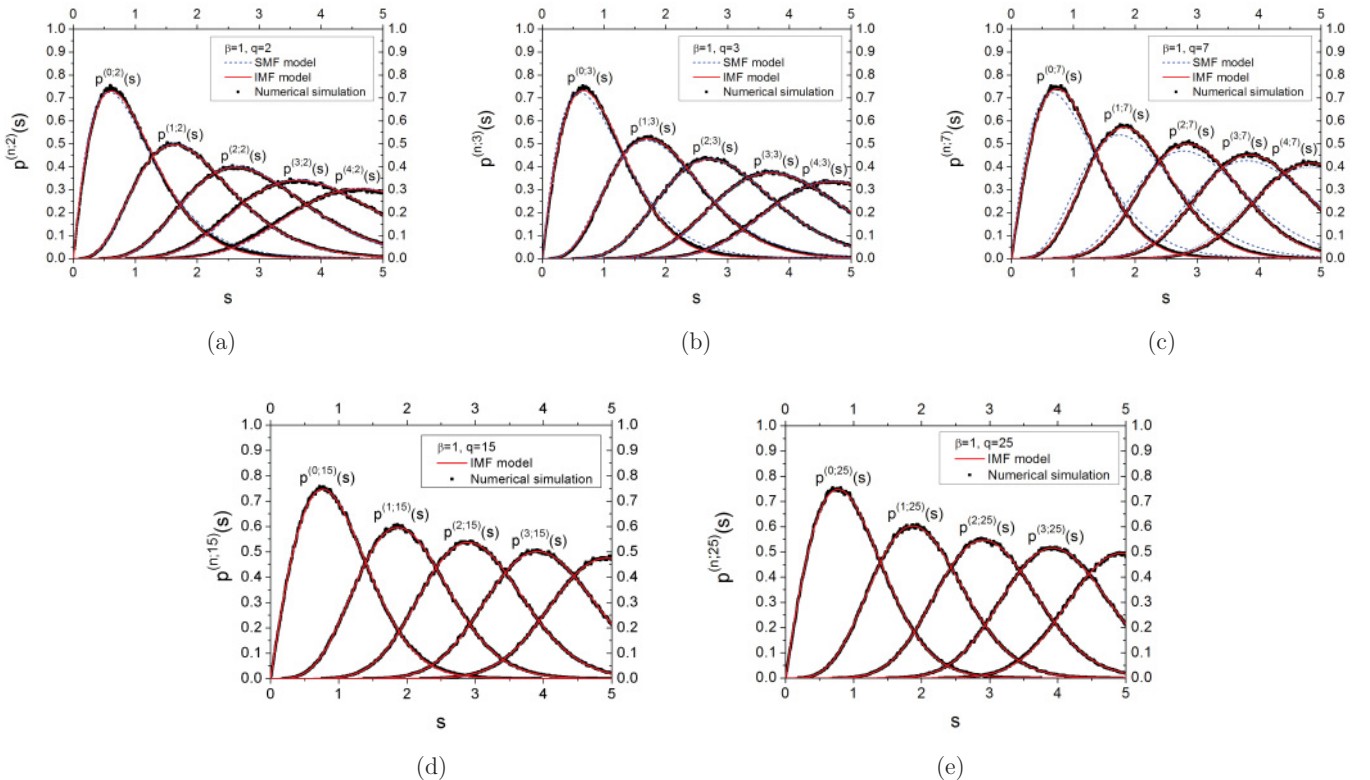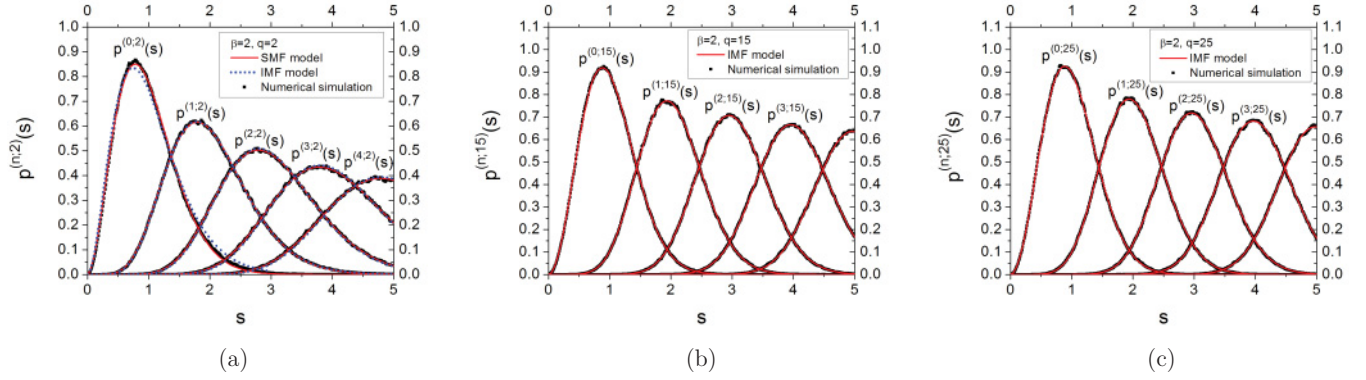

FIG. 3. (Color online) Comparison of SMF and IMF models with simulated data, for $\beta = 1$, for interactions spanning the range q from nearest neighbors to essentially infinite, viz., values of q of (a) 2, (b) 3, (c) 7, (d) 15, and (e) 25.

FIG. 4. (Color online) SMF and IMF models, with $\beta = 2$, for ranges of interaction $q = 2$, 15, and 25.

corresponds to a generalization for the case of finite-range interactions.

Second, the capture zone (CZ) distribution of islands generated in the early stages of epitaxial growth was modeled excellently by using the functional form given by Eq. (44) [41]. There, the authors use the maximum entropy method to justify this functional form as an approximation to the CZ distribution.

Finally, Eq. (44) has the same functional form as Eq. (4.1) in Ref. [42], where this expression is proposed for Dyson's Brownian motion model with $0 < \beta \leqslant 4$ based on heuristic arguments and on the asymptotic form found by Dyson for $p^{(0;\infty)}(s)$ [31]. They found that Eq. (44) gives good results for Dyson's Brownian motion model with a full range of interactions (for the values of β mentioned previously) [42]. From our results, this asymptotic form can clearly be interpreted as a mean-field approximation for Dyson's Brownian motion model for large values of q.

We emphasize that Eq. (44) is a generalization of the Wigner surmise for finite-range interactions, which seems to be related to many different models.

B. Spacing distribution functions for arbitrary-range interactions

For arbitrary interaction range, the analytic expression for the nth spacing distribution function is not so clear. The spacing distribution functions in the limit $s \to 0$ have the form

$$p^{(n;q)}(s) \propto s^{\alpha_n}, \qquad (46)$$

where α_n is a function of β, n, and q. From Eq. (12) it is possible to find this exponent by arguments similar to those used in Ref. [39] for the CRW case (see Appendix B).

However, for Dyson's Brownian motion model it is necessary to distinguish between the two cases $n < q - 1$ and $n \geqslant q - 1$. For the first, we find

$$\alpha_n = \frac{\beta \, (n + 1)(n + 2)}{2} + n, \qquad (47)$$

which is the same exponent as for random-matrix ensembles and Dyson's Brownian motion model with $q \to \infty$ and $\beta = 1$, 2, or 4. However, for $n \geqslant q - 1$ we find

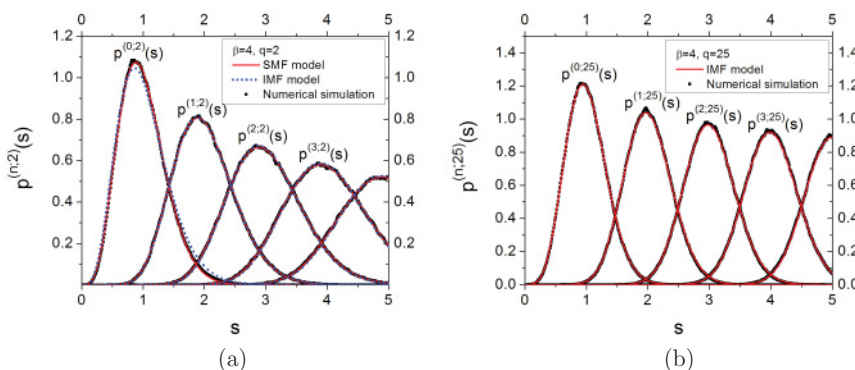$$\alpha_n = \frac{\beta \, q \, (3 + 2n - q)}{2} + n, \qquad (48)$$

differing from its counterpart in random matrices. Hence, the SMF model for arbitrary values of n can be written as

$$p^{(n;q)}(s) = A \, s^{\alpha_n} e^{-\beta \, C_1^n \, H_q \, s} \prod_{j=1}^{q-1} (s + j)^{\beta}, \qquad (49)$$

while the IMF model is given by

$$p^{(n;q)}(s) = A_n \, s^{\alpha_n} e^{-\beta \frac{\bar{C}_1^n}{2} \left(\frac{q-1}{q} \right) \frac{s^2}{\langle s^2 \rangle_n} - \beta \frac{\bar{C}_1^n}{q} s}, \qquad (50)$$

where α_n is defined by Eqs. (47) or (48). The results of the SMF and IMF models for $\beta = 1$, 2, and 4 are shown in Figs. 3, 4, and 5, respectively. In general, the IMF model gives better results than the SMF model. However, for large n and small q, both give similar results [see Figs. 4(a) and 5]. The SMF model describes the spacing distribution functions reasonably well for small values of q and β [see Figs. 3(a), 3(b), and 4(a)]. However, as expected from discussion at the beginning in Sec. V A 2, the SMF model gives poor results for higher values of q and β, as shown in Fig. 3(c). In general, the IMF gives good

FIG. 5. (Color online) SMF and IMF models for small and large interaction range, with $\beta = 4$.
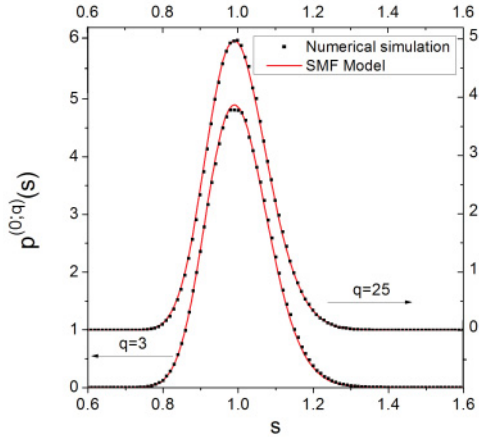
FIG. 6. (Color online) The SMF model for a set of particles which interact via $v(s) \propto s^{-2}$, with $q = 3$ and offset upward one unit $q = 25$. In both cases, we used $\beta = 1$ in the numerical simulation.

results. For large values of q, the IMF model gives excellent results, even for large values of n, at least for $\beta = 1, 2$, and 4. However, for small values of q and $\beta = 2,4$, Figs. 4(a) and Figs. 5(a) show that it gives good results only for small n. Both the SMF and IMF models give the exact statistical behavior of the system in the case $q = 1$, while for full-range interactions, only the IMF reduces to the EWS.

C. Another example: TSK model

Vicinal crystals usually have terraces oriented in the high-symmetry direction separated by steps of atomic height; see, for example, Ref. [43]. The terrace-width distribution (TWD) of vicinal surfaces, that is, the distribution of separations between adjacent steps, has special interest for experimentalists because it gives information about the the interaction between steps [24]. It is assumed that the steps cannot cross each other and, in the simplest case of the TSK model, that the dominant excitation is the formation of kinks. Typically, the step edges interact via a pair potential $v(x)$, where x is the distance between the steps. Usually, the elastic and entropic contributions to the step-step interactions take the form $v(x) = \mathcal{A} x^{-2}$. In Refs. [40] and [44], it was shown that this kind of potential gives a good description of the TWD for interacting steps. That is our motivation for extending our SMF model to this potential. We used the same approximation made in the previous section but now with this potential, finding that

$$p^{(0;q)}(s) = A \, e^{-\beta \mathcal{A} C_3 H_q^3 s - (\beta/2)\mathcal{A} \sum_{j=1}^{q}[s+(j-1)]^{-2}}. \quad (51)$$

The functional form of the SMF model is similar to the one of the zeroth-order model proposed in Ref. [40]. Figure 6(b) shows that Eq. (51) accounts well for the numerical data. Remarkably, in spite of its simplicity, the SMF approximation describes $p^{(0;q)}(s)$ very well even for large q.

VI. CONCLUSION

In many cases, our knowledge about the statistical behavior of a many-particle system is reduced to the spacing distribution functions due to our inability to obtain numerically, experimentally, or analytically the joint distribution function $P_N(x_1, \ldots, x_N; \beta)$. Since the information contained in $p^{(0;q)}(s)$ is very limited, $p^{(n;q)}(s)$ with $n > 0$ should also be calculated to obtain additional physical information about the system.

In the IIA, the statistical behavior of the system is completely determined by $p^{(0;q)}(s)$. This is a crude approximation which becomes exact only in the case of nearest-neighbor interactions. However, we showed that the IIA can be applied satisfactorily in many cases. One of these cases is Dyson's Brownian motion model for small values of q. In this case, we expect that the correlations between gap sizes are weak, justifying the use of the IIA. Naturally, for large values of q the IIA gives poor results. We found also that the IIA—with a suitable choice of $p^{(0;q)}(s)$—is a reasonable approximation for $p^{(n;q)}(s)$ in the point island model for epitaxial growth, at least in 1D and 2D.

The EWS can be applied in systems where $p^{(n;q)}(s)$ can be characterized by its behavior in the limits $s \ll 1$ and $s \gg 1$. These are the cases of Dyson's Brownian motion model with $q = 1$ and $q = N - 1 \to \infty$. However, the EWS does not give good results for this model in the case of $1 < q < N - 1$. The EWS can also be used satisfactorily in the case of the 2D epitaxial growth mentioned previously.

The mean-field approximation proposed in this paper is a general tool to study classical interacting particles with finite or full interaction range. The SMF and IMF models are more general approximations than the IIA or the EWS. In particular, the IMF model given by Eq. (50) can be interpreted as a generalization of the EWS for a finite range of interaction. Additionally, the functional form of Eq. (44) can be used in different contexts [41,42], suggesting that this kind of model is related with other models for different systems.

In order to generalize the SMF and IMF models for $n > 0$ in Dyson's Brownian model, we calculated explicitly α_n from the results given in Ref. [1]. We found that one of the effects of the finite range of interactions is to change α_n. For $n < q - 1$, α_n has the same functional form of the case of complete range of interactions and it does not depend on q. For the case $n \geqslant q - 1$, we found a q dependence in α_n.

The IMF gives a good description of the Dyson's Brownian motion model, at least for $\beta = 1, 2$, and 4. In spite of their simplicity, the SMF and IMF models give excellent results for different kinds of interaction potentials. In particular, we also tested the SMF approximation for the potential $v(r) = \mathcal{A}/s^2$ of interacting steps.

APPENDIX A: MEAN-FIELD APPROXIMATION

As a first approximation, we replace $S_n \to \langle S \rangle = L/N$ for $n \neq m$. In this spirit, the average value over the ensemble of

particles at time t of the quotients in Eq. (32) can be written as

$$\left\langle \frac{1}{\sum_{i=1}^{j} S_{m\pm i}} \right\rangle \rightarrow \frac{C_1}{j\langle S \rangle} \tag{A1}$$

and

$$\left\langle \frac{1}{S_m + \sum_{i=1}^{j-1} S_{m\pm i}} \right\rangle \rightarrow \frac{C_2}{S + (j-1)\langle S \rangle}, \tag{A2}$$

where C_1 and C_2 are constants. Naturally, these constants can be interpreted as a renormalization of the strength of the interaction between particles.

We formulate an improved mean-field model by analyzing more carefully the dependence on S_m in Eq. (32). Following Refs. [22] and [23], we write

$$\left\langle \frac{S_m}{(x_{m+j+1} - x_{m+1})(x_{m+j+1} - x_m)} \right\rangle \rightarrow \varsigma_1(S), \tag{A3}$$

$$\left\langle \frac{S_m}{(x_m - x_{m-j})(x_{m+1} - x_{m-j})} \right\rangle \rightarrow \varsigma_1(S), \tag{A4}$$

where $\varsigma_1(S) = \tilde{C}_1 S/(j(j+1)\langle S^2 \rangle)$. Note that, in general, $\langle S^2 \rangle$ is a function of t. However, in our mean-field approach the average of S^2 at time t is replaced by the average in the stationary state $\langle \cdots \rangle_{\text{st}}$. In order to simplify our notation, in the text we omit the subscript indicating stationary state. In the same way, we write

$$\left\langle \frac{1}{x_{m+j+1} - x_{m+1}} \right\rangle = \left\langle \frac{1}{x_m - x_{m-j}} \right\rangle \rightarrow \varsigma_2(S), \tag{A5}$$

with $\varsigma_2(S) = \tilde{C}_1/(j\langle S \rangle)$. Finally, we use

$$\left\langle \frac{1}{S_m} \right\rangle \rightarrow \frac{\tilde{C}_2}{S}. \tag{A6}$$

Again, $\tilde{C}_1$ and $\tilde{C}_2$ are constants.

APPENDIX B: EXACT BEHAVIOR OF DYSON'S BROWNIAN MOTION MODEL FOR $s \ll 1$

From Eqs. (66) and (67) of Ref. [1], one can find the behavior of $p^{(n;q)}(s)$ for small values of s. The case $n < q - 1$ is given by Eq. (66) of Ref. [1]. Since $\sum_i^{n+1} S_i \ll \langle S \rangle$, we find

$$P_{n+1}(S_1, \ldots, S_{n+1}) \propto \int_0^\infty dS_{n+2} \ldots \int_0^\infty dS_{q-1} \zeta(\vec{S})\vartheta(\vec{S}), \tag{B1}$$

where

$$\zeta(\vec{S}) = \prod_{i=1}^{q-1} S_i^\beta \prod_{i=1}^{q-2} (S_i + S_{i+1})^\beta \ldots (S_i + \cdots + S_{q-1})^\beta \tag{B2}$$

and

$$\vartheta(\vec{S}) = \exp\left(-\frac{q\beta + 1}{\langle S \rangle} \sum_{j=1}^{q-1} S_j \right). \tag{B3}$$

After integration, Eq. (B1) reduces to

$$P_{n+1}(S_1, \ldots, S_{n+1}) \propto \prod_{i=1}^{n+1} S_i^\beta \prod_{i=1}^{n} (S_i + S_{i+1})^\beta \times \cdots$$
$$\times (S_1 + \cdots + S_{n+1})^\beta \vartheta(\vec{S}). \tag{B4}$$

Finally, using Eq. (B4) with Eq. (12) we find

$$p^{(n;q)}(s) \propto s^{n+\sum_{i=0}^{n}(n+1-i)} \propto s^{\frac{\beta(n+1)(n+2)}{2}+n}. \tag{B5}$$

For $n \geqslant q - 1$, we use Eq. (67) of Ref. [1]. Then

$$P_{n+1}(S_1, \ldots, S_{n+1}) \propto \prod_{j=1}^{q-1} \prod_{i=1}^{n+1-j} (S_i + \cdots + S_{i+j})^\beta. \tag{B6}$$

Substituting Eq. (B6) into Eq. (12) leads to

$$p^{(n;q)}(s) \propto s^{\beta \sum_{j=0}^{q-1}(n-j+1)+n} = s^{\frac{q}{2}(3+2n-q)\beta+n}. \tag{B7}$$

[1] E. Bogomolny, U. Gerland, and C. Schmit, Eur. Phys. J. B **19**, 121 (2001).

[2] Z. W. Salsburg, R. W. Zwanzig, and J. G. Kirkwood, J. Chem. Phys. **21**, 1098 (1953).

[3] P. J. Forrester, J. Phys. A: Math. Gen. **23**, 1259 (1990).

[4] D. ben-Avraham and E. Brunet, J. Phys. A. **38**, 3247 (2005).

[5] C. Doering, Phys. A (Amsterdam) **188**, 386 (1992).

[6] D. ben-Avraham, Phys. Rev. Lett. **81**, 4756 (1998).

[7] P. A. Alemany and D. ben-Avraham, Phys. Lett. A **206**, 18 (1995).

[8] J. Mettetal, B. Schmittmann, and R. Zia, Europhys. Lett. **58**, 653 (2002).

[9] S. J. Cornell and A. J. Bray, Phys. Rev. E **54**, 1153 (1996).

[10] V. Spirin, P. L. Krapivsky, and S. Redner, Phys. Rev. E **60**, 2670 (1999).

[11] B. Derrida and R. Zeitak, Phys. Rev. E **54**, 2513 (1996).

[12] D. L. González and G. Téllez, Phys. Rev. E **76**, 011126 (2007).

[13] F. D. A. Aarão Reis and R. B. Stinchcombe, Phys. Rev. E **71**, 026110 (2005).

[14] B. Derrida, C. Godrèche, and I. Yekutieli, Phys. Rev. A **44**, 6241 (1991).

[15] D. L. González and G. Téllez, in *Traffic and Granular Flow '07*, edited by C. Appert-Rolland, F. Chevoir, P. Gondret, S. Lassarre, J.-P. Lebacque, and M. Schreckenberg (Springer, Berlin, 2009).

[16] M. L. Mehta, *Random Matrices*, 3rd ed. (Elsevier, Amsterdam, 2004).

[17] A. Y. Abul-Magd and M. H. Simbel, Phys. Rev. E **60**, 5371 (1999).

[18] G. Auberson, S. R. Jain, and A. Khare, J. Phys. A **34**, 695 (2001).

[19] N. Kitanine, J. M. Maillet, N. A. Slavnov, and V. Terras, J. Phys. A: Math. Gen. **35**, L753 (2002).

[20] C. Mejía-Monasterio, T. Prosen, and G. Casati, Europhys. Lett. **72**, 520 (2005).

[21] D. L. Kaufman, I. Kosztin, and K. Schulten, Am. J. Phys. **67**, 133 (1999).

[22] A. Pimpinelli, H. Gebremariam, and T. L. Einstein, Phys. Rev. Lett. **95**, 24 (2005).

[23] A. BH. Hamouda, A. Pimpinelli, and T. L. Einstein, Surface Sci. **602**, 3569 (2008).

[24] T. L. Einstein, Appl. Phys. A **87**, 375 (2007).

[25] J. A. Blackman and P. A. Mulheran, Phys. Rev. B **54**, 11681 (1996).

[26] D. ben-Avraham and S. Havlin, *Diffusion and Reactions in Fractals and Disordered Systems* (Cambridge University Press, Cambridge, 2000).

[27] In Ref. 39, this was called the generalized Wigner surmise, with the generalization being to $n > 0$. Here we call this feature "extended," similar to Ref. 17, to avoid confusion with the generalized Wigner surmise discussed in Refs. [22–24] and [33], where the generalization is of the value of β to other than 1, 2, or 4.

[28] D. Chandler, *Introduction to Modern Statistical Mechanics* (Oxford University Press, Oxford, 1987).

[29] J. P. Hansen and I. R. McDonald, *Theory of Simple Liquids*, 2nd ed. (Academic Press, London, 1986).

[30] F. Dyson, J. Math. Phys. **3**, 140 (1962).

[31] F. Dyson, J. Math. Phys. **3**, 157 (1962).

[32] F. Shi, Y. Shim, and J. G. Amar, Phys. Rev. E **79**, 011602 (2009).

[33] A. Pimpinelli and T. L. Einstein, Phys. Rev. Lett. **99**, 226102 (2007).

[34] M. Li, Y. Han, and J. W. Evans, Phys. Rev. Lett. **104**, 149601 (2010).

[35] A. Pimpinelli and T. L. Einstein, Phys. Rev. Lett. **104**, 149602 (2010).

[36] Here, $p^{(n;\infty)}(s)$ is the probability that, given a particle at the center of a circle with radius s, there is another particle within an annulus centered at the first particle with internal radius s and external radius $s + ds$. The condition that there are n additional particles inside the disk of radius s still applies.

[37] D. Zhong and D. ben-Avraham, J. Phys. A **28**, 33 (1995).

[38] F. Haake, *Quantum Signatures of Chaos*, 3rd ed. (Springer, Berlin, 2010).

[39] D. L. González and G. Téllez, J. Stat. Phys. **132**, 187 (2008).

[40] P. N. Patrone, T. L. Einstein, and D. Margetis, Phys. Rev. E **82**, 061601 (2010).

[41] D. L. González, A. Pimpinelli, and T. L. Einstein, Phys. Rev. E **84**, 011601 (2011).

[42] R. Scharf and F. M. Izrailev, J. Phys. A **23**, 963 (1990).

[43] H.-C. Jeong and E. D. Williams, Surf. Sci. Rep. **34**, 171 (1999); M. Giesen, Prog. Surface Sci. **68**, 1 (2001).

[44] J. A. Yancey, H. L. Richards, and T. L. Einstein, Surface Sci. **598**, 78 (2005).